Computers and Concrete, *Vol. 16, No. 2 (2015) 329-342*
DOI: http://dx.doi.org/10.12989/cac.2015.16.2.329

A general tangent operator applied to concrete using a multi-surface plasticity model

Ana Beatriz C.G. Silva, Jose Claudio F. Telles,
Eduardo M.R. Fairbairn* and Fernando Luiz B. Ribeiro

Laboratory of Structures and Materials, Civil Engineering Programme, Federal University of Rio de Janeiro, Centro de Tecnologia, Ilha do Fundão, CEP 21945-970, Rio de Janeiro, Brazil

(Received November 1, 2014, Revised July 31, 2015, Accepted August 4, 2015)

Abstract. The present paper aims at developing a method to accommodate multi-surface concrete plasticity from the point of view of a consistency concept applied to general tangent operators. The idea is based on a Taylor series expansion of the actual effective stress at the stress point corresponding to the previous accumulated true stresses plus the current increment values, initially taken to be elastic. The proposed algorithm can be generalized for any multi-surface criteria combination and has been tested here for typical cement-based materials. A few examples of application are presented to demonstrate the effectiveness of the multi-surface technique as used to a combination of Rankine and Drucker-Prager yield criteria.

Keywords: finite element method; multi-surface plasticity; tangent operators; cement-based materials; concrete

1. Introduction

Elastoplastic problems are typically worked out by finite elements using Newton's like methods, in which a number of linear problems are sequentially solved. For rate-independent plasticity, the most commonly adopted numerical technique is the return mapping method proposed by Wilkins (1964). The classic operator methodology is based on an elastic prediction and a plastic correction. Different formulations have been proposed and extended to several constitutive equations models, comprising inelastic behavior, as can be seen in Krieg and Krieg (1977), Simo and Taylor (1985), Hofstetter *et al.* (1993) and Crisfield (1997).

Many works have used typical return mapping ideas in elastoplastic problems. Peng and Chen (2012) generalized the return mapping algorithm for isotropic plasticity in the principal stress space and Kassiotis *et al*. (2012) studied the stability and convergence parameters of particular plasticity cases. Even though these algorithms can be efficient for certain criteria, an adaptation procedure is still required to model materials with pronounced differences between compression and tension behavior. Such a behavior is found in cement-based materials and cannot be described

* Corresponding author, Professor, E-mail: eduardo@coc.ufrj.br

http://www.techno-press.org/?journal=cac&subpage=8 ISSN: 1598-8198 (Print), 1598-818X (Online)

by single surface plasticity models.

Concrete behavior in compression may be described by a single yield surface, whereas for tension, alternative models need to be used. Most of the research involving concrete models combines a single yield surface with a fracture model (Galic *et al.* 2011, Cervenka and Papanikolaou 2008, Grassl and Jirasek 2002, Benkemoun *et al.* 2011), but evidence has shown that degradation due to tensile cracking can be negligible when tensile cracking is not yet fully developed (Feenstra and De Borst 1995).

As an alternative procedure, Miers and Telles (2004) extended the concept of tangent operator without need for any yield criteria particularization. Although developed for boundary element analysis, this concept is the basis of the present work, which is here expanded to implicit elastoplastic finite element solution schemes including multi-surface criteria.

In this paper a return mapping algorithm for multi-surface plasticity is presented. The algorithm is quite general and can be specified including different yield criteria. Herein, *Rankine* and *Drucker-Prager* surfaces, commonly used in concrete plasticity problems, have been adopted to solve the examples discussed.

2. Constitutive equations

Within the context of small strains, isotropic material behavior and applying standard Cartesian tensor notation for Roman letter subscripts, the total strain tensor ε_{ij} is assumed to be decomposed into elastic and plastic components

$$\varepsilon_{ij} = \varepsilon_{ij}^{e} + \varepsilon_{ij}^{p} \tag{1}$$

where ε_{ij}^{e} is the elastic strain tensor and ε_{ij}^{p} the plastic strain tensor.

In general, plastic behavior existence depends on the following condition

$$F(\sigma_{ij}, k) = f(\sigma_{ij}) - \psi(k) = 0 \tag{2}$$

where $f(\sigma_{ij})$ is a scalar function of stress that can also be considered as an equivalent or effective stress σ_e, σ_{ij} is the stress tensor, k is the work hardening parameter and ψ represents here the uniaxial yield stress.

Considering the work hardening hypothesis, an effective plastic strain ε_e^p can be defined as an equivalent strain whose increment produces an increase in the plastic strain energy as

$$\sigma_e d\varepsilon_e^p = \sigma_{ij} d\varepsilon_{ij}^p = dk \tag{3}$$

To obtain the stress-strain relationship, this hardening hypothesis can be used as follows

$$d\sigma_{ij} = C_{ijkl}\left(d\varepsilon_{kl} - d\varepsilon_{kl}^{p}\right) \tag{4}$$

where C_{ijkl} denotes the fourth-order tensor of elastic constants.

Within the context of associated plasticity, the normality principle can be written as

$$d\varepsilon_{ij}^{p} = d\lambda \frac{\partial F}{\partial \sigma_{ij}} \tag{5}$$

in which $d\lambda$ is a proportionality factor known as plastic multiplier. The substitution of Eq. (5) in Eq. (4) results in

$$d\sigma_{ij} = C_{ijkl}\left(d\varepsilon_{kl} - a_{kl}d\lambda\right) \tag{6}$$

Where

$$a_{kl} = \frac{\partial F}{\partial \sigma_{ij}} \tag{7}$$

The flow function differentiation leads to

$$dF = a_{ij}d\sigma_{ij} - \frac{d\psi}{dk}dk = 0 \tag{8}$$

or

$$dF = a_{ij}d\sigma_{ij} - \frac{d\psi}{dk}\sigma_{ij}d\varepsilon_{ij}^{p} = 0 \tag{9}$$

Applying the normality principle, one obtains

$$a_{ij}d\sigma_{ij} - \frac{d\psi}{dk}\sigma_{ij}a_{ij}d\lambda = 0 \tag{10}$$

Substituting Eq. (6) in the above expression and solving for $d\lambda$ results in

$$d\lambda = \frac{1}{\gamma'}a_{ij}C_{ijkl}d\varepsilon_{kl} \tag{11}$$

where

$$\gamma' = a_{ij}C_{ijkl}a_{kl} + \frac{d\psi}{dk}\sigma_{ij}a_{ij} \tag{12}$$

and since $f(\sigma_{ij})$ is homogeneous of first order,

$$\sigma_{ij}\frac{\partial f}{\partial \sigma_{ij}} = f(\sigma_{ij}) = \sigma_{e} \tag{13}$$

Substituting Eqs. (3)-(13) in Eq. (12)

$$\gamma' = a_{ij}C_{ijkl}a_{kl} + \frac{d\psi}{d\varepsilon_{e}^{p}} \tag{14}$$

where

$$\frac{d\psi}{d\varepsilon_e^p} = H' \tag{15}$$

with H' being the slope of the uniaxial curve plotted as stress versus plastic strain. Here, negative strain-softening behavior can be accommodated, provided scale dependency is properly taken into account (Lackner and Mang 2004).

Eq. (11) can now be used to substitute for $d\lambda$ in Eq. (6) to generate the required incremental stress-strain relations

$$d\sigma_{ij} = C_{ijkl}^{ep}\, d\varepsilon_{kl} \tag{16}$$

For improved computer efficiency, Eq. (16) can be further manipulated to allow for computation of true stress increments as a function of "elastic" or fictitious stress increments $d\sigma_{ij}^e$ in the form

$$d\sigma_{ij} = d\sigma_{ij}^e - \frac{1}{\gamma'} C_{ijmn} a_{mn} a_{op} d\sigma_{op}^e \tag{17}$$

Where

$$d\sigma_{ij}^e = C_{ijkl}\, d\varepsilon_{kl} \tag{18}$$

3. Implementation procedures

3.1 Single surface criteria

Starting with the general conditions describing the plastic behavior, computed values of stress and internal variables must satisfy a Taylor series expansion of the consistency condition described by Eq. (2). Hence,

$$F(f,\psi)\big|_{\sigma_{ij}+\Delta\sigma_{ij}} \cong F(f,\psi)\big|_{\sigma_{ij}+\Delta\sigma_{ij}^e} + \left.\frac{\partial F(f,\psi)}{\partial \varepsilon_{ij}^p}\right|_{\sigma_{ij}+\Delta\sigma_{ij}^e} \cdot \Delta\varepsilon_{ij}^p + \ldots = 0 \tag{19}$$

where $\Delta\sigma_{ij}^e$ is the current (trial) "elastic" stress increment, σ_{ij} is the accumulated true stress from the previous load history and iterations and $\Delta\varepsilon_{ij}^p$ is the current plastic strain increment.

Substituting Eq. (2) for the derivative of F in Eq. (19) leads to

$$\frac{\partial F(f,\psi)}{\partial \varepsilon_{ij}^p} = \frac{\partial f}{\partial \varepsilon_{ij}^p} - \frac{\partial \psi}{\partial \varepsilon_{ij}^p} = -C_{ijkl} a_{kl} - \frac{\partial \psi}{\partial \varepsilon_{ij}^p} \tag{20}$$

And

$$\frac{\partial \psi}{\partial \varepsilon_{ij}^{p}} = \frac{\partial \psi}{\partial \varepsilon_{e}^{p}} \cdot \frac{\partial \varepsilon_{e}^{p}}{\partial \varepsilon_{ij}^{p}} = H' \frac{\sigma_{ij}}{\sigma_{e}} \tag{21}$$

Thus, substituting Eqs. (20) and (21) in Eq. (19) lead to

$$F(f,\psi)\big|_{\sigma_{ij}+\Delta\sigma_{ij}^{e}} - \left(C_{ijkl} a_{kl} + H' \frac{\sigma_{ij}}{\sigma_{e}} \right) \Delta\varepsilon_{ij}^{p} = 0 \tag{22}$$

So,

$$F(f,\psi)\big|_{\sigma_{ij}+\Delta\sigma_{ij}^{e}} - \left(C_{ijkl} a_{kl} + H' \frac{\sigma_{ij}}{\sigma_{e}} \right) a_{ij} \Delta\lambda = 0 \tag{23}$$

or remembering Eq. (13)

$$F(f,\psi)\big|_{\sigma_{ij}+\Delta\sigma_{ij}^{e}} - \left(a_{ij} C_{ijkl} a_{kl} + H' \right) \Delta\lambda = 0 \tag{24}$$

Finally, Eq. (24) can be reordered

$$\Delta\lambda = \left. \frac{F(f,\psi)\big|_{\sigma_{ij}+\Delta\sigma_{ij}^{e}}}{\left(a_{ij} C_{ijkl} a_{kl} + H' \right)} \right|_{\sigma_{ij}+\Delta\sigma_{ij}^{e}} \tag{25}$$

and the current true stress increment $\Delta\sigma_{ij}$, to be accumulated, can be calculated as

$$\Delta\sigma_{ij} = \Delta\sigma_{ij}^{e} - \Delta\lambda\, C_{ijkl}\, a_{kl}\big|_{\sigma_{ij}+\Delta\sigma_{ij}^{e}} \tag{26}$$

For the new iteration, adopting $d_{ij} = C_{ijkl}\, a_{kl}$, the plastic multiplier is defined as follows,

$$\Delta\lambda = \left. \frac{F(f,\psi)\big|_{\sigma_{ij}+\Delta\sigma_{ij}}}{\left(a_{ij} d_{ij} + H' \right)} \right|_{\sigma_{ij}+\Delta\sigma_{ij}} \tag{27}$$

Iterations are carried out until $F(f,\psi) \cong 0$ is obtained within a prescribed tolerance.

3.2 Multi-surface criteria

Solving the problem for two surfaces, the previous equations can be rewritten assuming that there are two yield conditions $F_1(f_1,\psi_1)$ and $F_2(f_2,\psi_2)$ which must be satisfied simultaneously. Hence, considering that the plastic strain increment can be defined as

$$\Delta\varepsilon_{ij}^{p} = a_{ij}^{1}\Delta\lambda^{1} + a_{ij}^{2}\Delta\lambda^{2} = \left(\Delta\varepsilon_{ij}^{p}\right)^{1} + \left(\Delta\varepsilon_{ij}^{p}\right)^{2} \tag{28}$$

the general yield condition $F_\alpha(f_\alpha,\psi_\alpha)$ can be expanded in Taylor series as follows

$$F_\alpha\big|_{\sigma_{ij}+\Delta\sigma_{ij}} \cong F_\alpha\big|_{\sigma_{ij}+\Delta\sigma_{ij}^e} + \left.\frac{\partial F_\alpha}{\partial\left(\varepsilon_{ij}^p\right)^1}\right|_{\sigma_{ij}+\Delta\sigma_{ij}^e} \cdot \left(\Delta\varepsilon_{ij}^p\right)^1 + \left.\frac{\partial F_\alpha}{\partial\left(\varepsilon_{ij}^p\right)^2}\right|_{\sigma_{ij}+\Delta\sigma_{ij}^e} \cdot \left(\Delta\varepsilon_{ij}^p\right)^2 + \ldots = 0 \tag{29}$$

But, similarly to Eq. (20), one has (summation not implied over repeated Greek letter indices)

$$\frac{\partial F_\alpha}{\partial\left(\varepsilon_{ij}^p\right)^\beta} = \frac{\partial f_\alpha}{\partial\left(\varepsilon_{ij}^p\right)^\beta} - \frac{\partial \psi_\alpha}{\partial\left(\varepsilon_{ij}^p\right)^\beta} = -C_{ijkl}\left(a_{kl}\right)^\alpha - \frac{H_\alpha^{'}}{\left(\sigma_e\right)^\beta}\sigma_{ij}\delta_{\alpha\beta} \tag{30}$$

where $\delta_{\alpha\beta}$ stands for the Kronecker delta symbol.

Thus,

$$\begin{aligned} F_\alpha\big|_{\sigma_{ij}+\Delta\sigma_{ij}} \cong F_\alpha\big|_{\sigma_{ij}+\Delta\sigma_{ij}^e} - \left(C_{ijkl}\left(a_{kl}\right)^\alpha + \frac{H_\alpha^{'}}{\left(\sigma_e\right)^1}\sigma_{ij}\delta_{\alpha 1}\right)\cdot\left(\Delta\varepsilon_{ij}^p\right)^1 - \\ \left(C_{ijkl}\left(a_{kl}\right)^\alpha + \frac{H_\alpha^{'}}{\left(\sigma_e\right)^2}\sigma_{ij}\delta_{\alpha 2}\right)\cdot\left(\Delta\varepsilon_{ij}^p\right)^2 = 0 \end{aligned} \tag{31}$$

or

$$\begin{aligned} F_\alpha\big|_{\sigma_{ij}+\Delta\sigma_{ij}} \cong F_\alpha\big|_{\sigma_{ij}+\Delta\sigma_{ij}^e} - \left(C_{ijkl}\left(a_{kl}\right)^\alpha\left(a_{ij}\right)^1 + \frac{H_\alpha^{'}}{\left(\sigma_e\right)^1}\sigma_{ij}\delta_{\alpha 1}\left(a_{ij}\right)^1\right)\cdot\left(\Delta\lambda\right)^1 - \\ \left(C_{ijkl}\left(a_{kl}\right)^\alpha\left(a_{ij}\right)^2 + \frac{H_\alpha^{'}}{\left(\sigma_e\right)^2}\sigma_{ij}\delta_{\alpha 2}\left(a_{ij}\right)^2\right)\cdot\left(\Delta\lambda\right)^2 = 0 \end{aligned} \tag{32}$$

which provides

$$\begin{aligned} F_\alpha\big|_{\sigma_{ij}+\Delta\sigma_{ij}^e} - \left(C_{ijkl}\left(a_{kl}\right)^\alpha\left(a_{ij}\right)^1 + H_\alpha^{'}\delta_{\alpha 1}\right)\cdot\left(\Delta\lambda\right)^1 - \\ \left(C_{ijkl}\left(a_{kl}\right)^\alpha\left(a_{ij}\right)^2 + H_\alpha^{'}\delta_{\alpha 2}\right)\cdot\left(\Delta\lambda\right)^2 = 0 \end{aligned} \tag{33}$$

Therefore, one obtains the following system of equations for the plastic multipliers

$$\begin{aligned} F_1\big|_{\sigma_{ij}+\Delta\sigma_{ij}^e} - \left(\left(d_{ij}\right)^1\left(a_{ij}\right)^1 + H_1^{'}\right)\cdot\left(\Delta\lambda\right)^1 - \left(\left(d_{ij}\right)^1\left(a_{ij}\right)^2\right)\cdot\left(\Delta\lambda\right)^2 = 0 \\ F_2\big|_{\sigma_{ij}+\Delta\sigma_{ij}^e} - \left(\left(d_{ij}\right)^2\left(a_{ij}\right)^1\right)\cdot\left(\Delta\lambda\right)^1 - \left(\left(d_{ij}\right)^2\left(a_{ij}\right)^2 + H_2^{'}\right)\cdot\left(\Delta\lambda\right)^2 = 0 \end{aligned} \tag{34}$$

and the current true stress increment $\Delta\sigma_{ij}$, to be accumulated, can be calculated as

$$\Delta\sigma_{ij} = \Delta\sigma_{ij}^e - \left[\left(\Delta\lambda\right)^1\left(d_{ij}\right)^1 + \left(\Delta\lambda\right)^2\left(d_{ij}\right)^2\right]\Big\|_{\sigma_{ij}+\Delta\sigma_{ij}^e} \tag{35}$$

As before, for each new iteration, system of Eq. (34) is solved again for $\left(\Delta\lambda\right)^1$ and $\left(\Delta\lambda\right)^2$ until

approximate satisfaction of the yield conditions is observed.

3.3 Concrete multi-surface plasticity

Concrete plasticity is commonly based on two different yield criteria, simultaneously applied. These are *Rankine* (Galic *et al*. 2010) for (tension) positive stress limitation, $\psi = f_t$ - uniaxial tensile strength, and *Drucker-Prager* (Lackner *et al*. 2002) for compression, $\psi = f_c$ - uniaxial compressive strength; they are defined as

$$\textit{Rankine:}\quad \sqrt{J_2}\left[\cos\theta - \frac{\sin\theta}{\sqrt{3}}\right] + \frac{I_1}{3} - \psi(k) = 0 \tag{36}$$

$$\textit{Drucker-Prager:}\quad \alpha\beta I_1 + \beta\sqrt{J_2} - \psi(k) = 0 \tag{37}$$

The stress invariants are calculated by

$$I_1 = \sigma_{kk} \tag{38}$$

$$J_2 = \frac{1}{2} S_{ij} S_{ij} \tag{39}$$

$$-\frac{\pi}{6} \le \theta = \frac{1}{3}\sin^{-1}\left(-\frac{J_3}{2}\left(\frac{3}{J_2}\right)^{\frac{3}{2}}\right) \le \frac{\pi}{6} \tag{40}$$

in which $S_{ij} = \sigma_{ij} - \frac{I_1}{3}\delta_{ij}$ and $J_3 = \frac{1}{3} S_{ij} S_{jk} S_{ki}$.

Also, the *Drucker-Prager* parameters α and β can be obtained by the following expressions

$$\alpha = \frac{\kappa - 1}{\sqrt{3}\left(2\kappa - 1\right)} \tag{41}$$

$$\beta = \frac{\sqrt{3}\left(2\kappa - 1\right)}{\kappa} \tag{42}$$

where the parameter κ is a constant defined as

$$\kappa = \frac{f_{bc}}{f_c} \tag{43}$$

and f_{bc} represents the biaxial compressive stress.

Rankine criterion is generally used in terms of its formulation in the principal-stress space due to its trivial geometric representation of three planes perpendicular to the reference axes. However, since this formulation demands laborious transformation of stresses from the general reference stress space to the principal-stress space (Lackner *et al.* 2002), it has not been adopted here.

In addition, another alternative criterion can also be adopted, as seen in the literature (Hofstetter *et al.* 1993, Hellmich *et al.* 1999), to substitute *Rankine*'s in the tension limitation range. This is the *Tension Cut-off* criterion defined as follows

Table 1 Multi-surface plasticity algorithm

1. One starts with the trial elastic stress $\Delta\boldsymbol{\sigma}^{e}$ assuming that the strain increment is elastic;
2. Initialize i = 0 (iteration number) and $\sigma_{n+1}{}^{0} = \sigma_n + \Delta\sigma^{e}_{n+1}$;
3. Calculate F_1 and F_2 and check convergence:
If $F_1 < 0$ and $F_2 < 0 \longrightarrow$ The trial elastic stress is the actual correct solution. Go to 7.
Elseif $F_1 \geq 0$ or $F_2 \geq 0 \longrightarrow$ Proceed as in a single surface algorithm for the surface activated during the iteration.
Elseif $F_1 \geq 0$ and $F_2 \geq 0 \longrightarrow$ Proceed to the multi-surface algorithm below;
4. Calculate the plastic multiplier $\Delta\lambda^{1^{i}}$ and $\Delta\lambda^{2^{i}}$;
5. Update solution $\sigma_{n+1}{}^{i+1} = \sigma_{n+1}{}^{i} - (\Delta\lambda^{1^{i}}(d^{1})^{i} + \Delta\lambda^{2^{i}}(d^{2})^{i})$;
6. Increase iteration counter: *i = i + 1* and go to 3.
7. End of algorithm.

$$I_1 - \psi(k) = 0 \tag{44}$$

The above criterion includes the influence of compression stresses, in the other stress planes, to simulate the tension cut-off behavior. Since this somewhat undesirable influence is not present in Rankine's, the latter has been found preferable for actual approximation of concrete behavior under mixed stress states.

Finally, the structure of the numerical solution algorithm at a generic load step n+1, considering the discussed multi-surface criteria, is described in Table 1.

4. Results

In order to validate the technique presented, a simple example was first developed to test the multi-surface plasticity formulation, in different stress situations, including the activation of two yield criteria simultaneously. Then, a simulation of the Brazilian split cylinder test has been carried out in plane strain, plane stress and in a full three-dimensional model. All examples have been solved using a general finite element program developed in the Laboratory of Structures and Materials of the Civil Engineering Programme of COPPE/UFRJ (Ribeiro and Ferreira 2007).

4.1 Theoretical return mapping test example

To assess the return mapping algorithm of the multi-surface plasticity model, a simple example was selected. The problem consists of a 3-D hexahedral geometry, measuring 1m x 1m x 1m, simply supported over three faces and subjected to a plane stress condition, as depicted in Fig. 1. Ideal plasticity has been assumed and solutions for different single step x and y prescribed displacements have been obtained. The main purpose has been to elastically violate the multi-surface (*Rankine* and *Drucker-Prager*) criterion under different 2-D stress conditions obtained by varying the imposed values of the prescribed displacements. Material properties are Young modulus 30.0 GPa, Poisson's ratio 0.2, compressive strength 30.0 MPa, tensile strength 3.0 MPa and biaxial compressive strength 36.0 MPa. The displacement imposed elastic solutions and the respective converged elastoplastic final stresses can be seen in Fig. 2. In all cases, entirely acceptable results, corresponding to satisfaction of the multi-surface criterion, have been obtained, also including elastic stress points violating the multi-surface right at the intersection of the Rankine and Drucker-Prager surfaces.

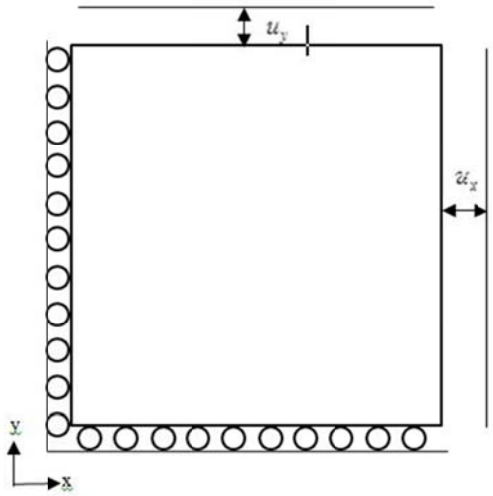

Fig. 1 Problem description

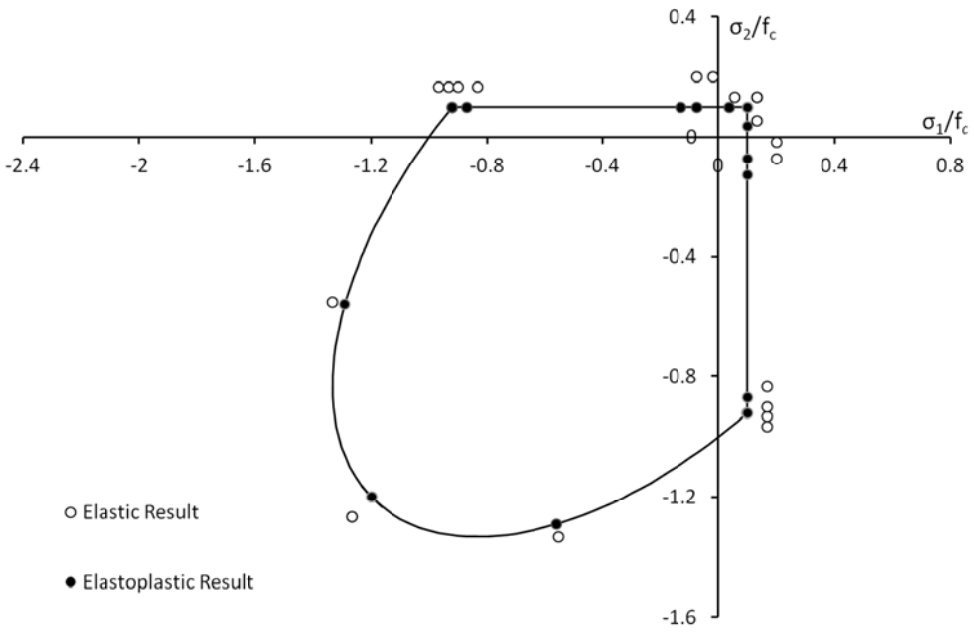

Fig. 2 Elastic and elastoplastic solutions

4.2 Brazilian split cylinder test

The Brazilian split cylinder test is an experiment in which a cylindrical specimen is diametrically compressed along its top and bottom generators until mid plane vertical diameter normal splitting is identified. It is internationally considered a standard method for assessing the

uniaxial tensile strength of concrete materials (e.g. Olesen *et al.* 2005). The loading of the cylinder produces a tensile stress normal to the loading plane inducing a mode one tension crack observed during the test (Rocco *et al.* 1999). Here, the multi-surface criterion has been used to model the behavior of the cylinder, including the discussed *Rankine* and *Drucker-Prager* criteria. In addition, since this is not a limit load analysis; i.e. the maximum load bearing, considerably higher than that required for cracking the vertical diameter, is dictated by the resistance to the vertical compression stresses, the experiment has been simulated by comparing the resultant applied load (or displacement for that matter) versus progress of the plastic zone over the vertical diameter surface area. Namely, the percentage of the diametral plane plastic area versus the total diametral plane area has been used to predict the experimental splitting, via the elastoplastic multi-surface criterion. Bearing in mind that the *Rankine* surface dominates the plastic zone evolution there, tension stress limitation is seen actively present in the numerical simulation.

Due to symmetry, the finite element model considers only a quarter of the cylinder (Fig. 3) with a 100.0 mm diameter (D), a length (L) of 200.0 mm and a loading strip ($2a$) of 10.0 mm. A threefold modeling strategy has been adopted, comprising plane strain, plane stress and three-dimensional models. After some trial convergence tests, the final mesh for the two-dimensional models was composed by 9405 four-node quadrilateral elements, as can be seen in Fig. 4(a). For the three-dimensional model 90168 eight-node hexahedral elements were adopted Fig. 4(b).

For the concrete material, a Young modulus of 30.0 GPa, a Poisson's ratio of 0.2, a tensile strength of 2.0 MPa, a uniaxial compression strength of 30.0 MPa and a biaxial compression strength of 36.0 MPa have been adopted. The loading strip is modeled as a linear elastic material with a young modulus of 1.0 GPa. To simulate the vertical load applied to the loading strip, vertical displacements at the top layer of the loading strip have been prescribed.

Fig. 5 shows the results of the split cylinder test for plane stress, plane strain and three-dimensional formulations. The horizontal axis indicates the prescribed displacement and at the average value of *u=0.08 to 0.1 mm,* the resultant vertical P load could be seen to match the theoretical value P_e (Olesen *et al.* 2005), defined as

$$P_e = \frac{f_t \pi D}{2L}\left[1-\left(\frac{2a}{D}\right)^2\right]^{-\frac{3}{2}} \tag{45}$$

Hence, at roughly 0.09 mm and at the onset of the horizontal 100% response, the resultant normalized vertical load was found to approach $P/P_e \cong 1.0$, as expected. As an illustration, the corresponding displacement versus vertical load curve is depicted in Fig. 6 to confirm the vertical compression load bearing capacity has not yet been achieved at $P/P_e \cong 1.0$.

The plastic zone evolution is presented in Figs. 7-9 for plane strain, plane stress and three-dimensional problems. A monochromatic scheme is used to represent the different yield criteria: light-gray represents the elastic zone, gray represents the *Ducker-Prager* plastic zone, dark-gray indicates violation of the two criteria simultaneously and black represents the single *Rankine* plastic zone. An interesting aspect of the three simulations is that over the mid length section of the 3-D results, good plane strain agreement can be observed, whereas plane stress behavior is clearly identified over the end extremities.

The plastic evolution for the three different models illustrate the exact moment when the

expected actual crack opening occurs (about *u=0.09 mm*), under the approximate unit normalized load, justifying the commonly observed splitting experimental results.

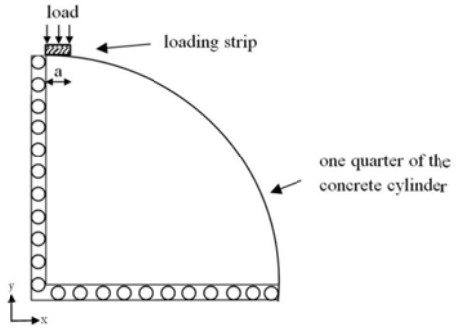

Fig. 1 Brazilian split cylinder model

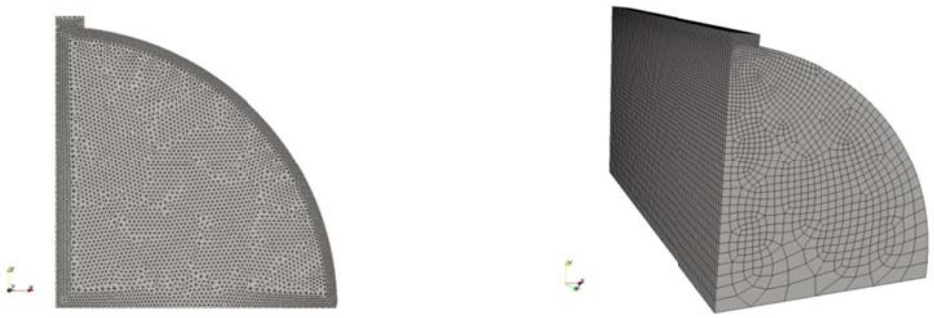

(a) Two dimensional mesh-9405 quadrilateral elements (b) Three-dimensional mesh-90168 hexahedral elements

Fig. 4 Problem mesh

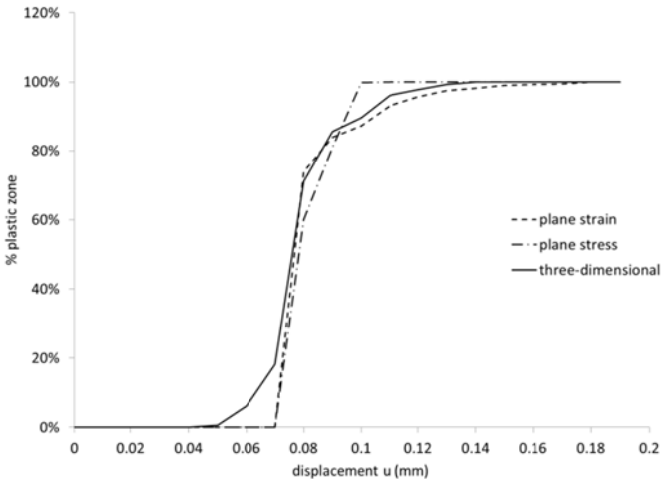

Fig. 5 Displacement *u* versus progress of the plastic zone over the vertical diameter surface area

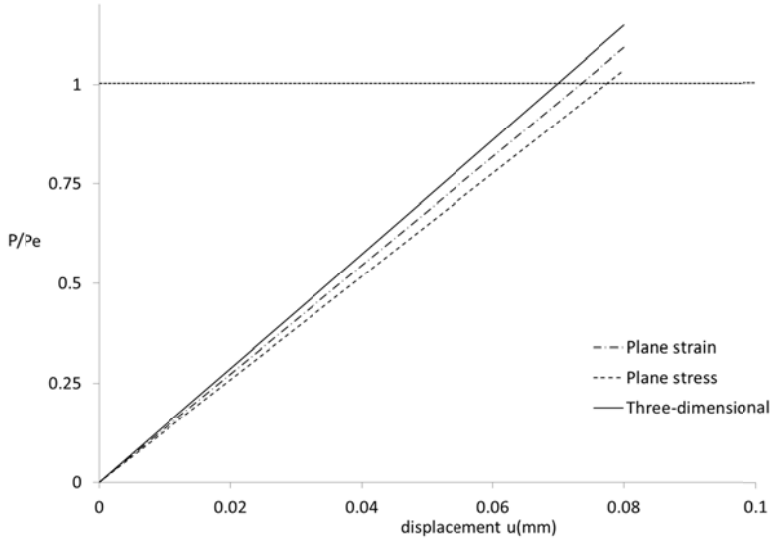

Fig. 6 Displacement *u* versus normalized vertical load P/P_e

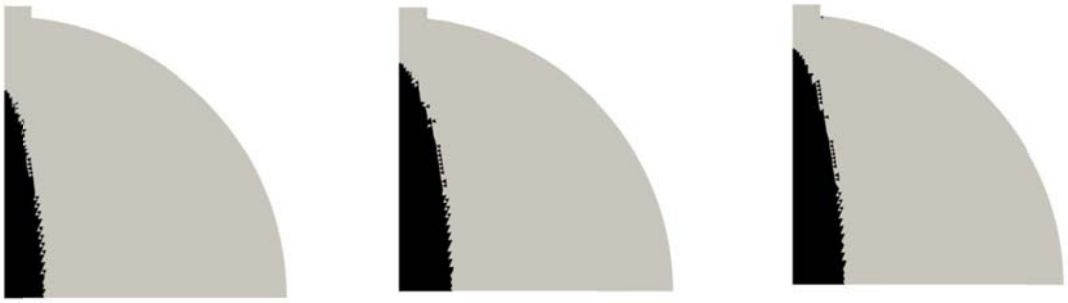

(a) Displacement u = 0.08 mm (b) Displacement u = 0.09 mm (c) Displacement u = 0.1 mm

Fig. 7 Results of plane strain problem

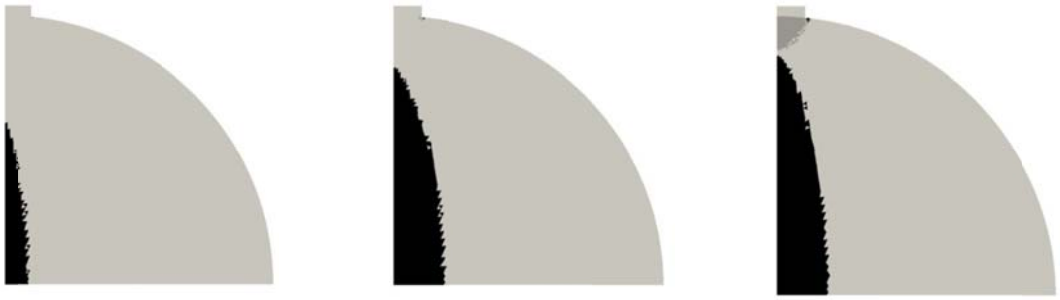

(a) Displacement u = 0.08 mm (b) Displacement u = 0.09 mm (c) Displacement u = 0.1 mm

Fig. 8 Results of plane stress problem

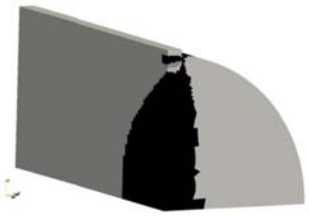

(a) Displacement u = 0.07 mm

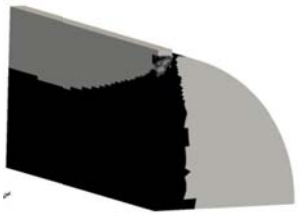

(b) Displacement u = 0.08 mm

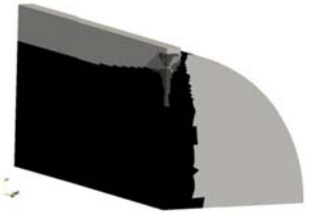

(c) Displacement u = 0.09 mm

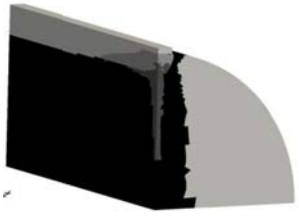

(d) Displacement u = 0.1 mm

Fig. 9 Results of the three-dimensional problem

5. Conclusions

In this work a return mapping algorithm applied to multi-surface concrete plasticity models has been presented. The developed algorithm is quite general and can be specified to different multi-surface yield criteria, including the alternative to simulate hardening/softening slopes, not included in the examples discussed here. Different test examples illustrate applications of the proposed technique to model concrete behavior under tensile and compressive stresses, using *Rankine* and *Drucker-Prager* yield criteria.

The proposed algorithm employs a general description of the Rankine criterion, in the standard current solution stress space, avoiding laborious transformations of stresses to the principal-stress space. Hence, the Rankine criterion is implemented in line with any other general yield criterion. Also, the proposed formulation demonstrated its robustness in the simulation of a problem, quite complex as the Brazilian splitting test, indicating good convergence for the several combinations of tensile and compressive stresses.

Acknowledgments

The authors thankfully acknowledge Petrobras for the financial support.

References

Benkemoun, N., Ibrahimbegovic, A. and Colliat, J.B. (2012), "Anisotropic constitutive model of plasticity capable of accounting for details of meso-structure of two-phase composite material", *Comput. Struct.*, **90-91**, 153-162.

Cervenka, J. and Papanikolaou, V.K. (2008), "Three dimensional combined fracture-plastic material model for concrete", *Int. J. Plasticity.*, **24**(12), 2192-2220.

Crisfield, M.A. (1997), *Non-Linear Finite Element Analysis of Solids and Structures. Advanced Topics*, Wiley, New York, USA.
Etse, G. and Willam, K. (1994), "Fracture energy formulation for inelastic behavior of plain concrete", *J. Eng. Mech. - ASCE*, **120**(9), 1983-2011.
Feenstra, P.H. and De Borst, R. (1996), "A composite plasticity model for concrete", *Int. J. Solids. Struct.*, **33**(5), 707-730.
Galic, M., Marovic, P. and Nikolic, Z. (2011), "Modified mohr-coulomb-rankine material model for concrete", *Mater. Model. Concrete.*, **28**(7), 853-887.
Grassl, P., Lundgren, K. and Gylltoft, K. (2002), "Concrete in compression: a plasticity theory with a novel hardening law", *Int. J. Solids. Struct.*, **39**, 5205-5223.
Hellmich, C., Ulm, F.J. and Mang, H.A. (1999), "Multisurface chemoplasticity. I: material model for shotcrete", *J. Eng. Mech.*, **125**(6), 692-701.
Hofstetter, G., Simo, J.C. and Taylor, R.L. (1993), "A modified cap model: closest point solution algorithms", *Comput. Struct.*, **46**(2), 203-214.
Krieg, R.D. and Krieg, D.B. (1977), "Accuracies of numerical solution methods for the elastic-perfectly plastic model", *J. Press. Vess. - T. ASME*, **99**, 510-515.
Lackner, R., Hellmich, C. and Mang, H.A. (2002), "Constitutive modeling of cementitious materials in the framework of chemoplasticity", *Int. J. Numer. Meth. Eng.*, **53**(10), 2257-2388.
Lackner, R. and Mang, H.A. (2004), "Chemoplastic material model for the simulation of early-age cracking: From the constitutive law to numerical analyses of massive concrete structures", *Cement. Concrete. Compos.*, **26**(5), 551-562.
Miers, L.S. and Telles, J.C.F. (2004), "A general tangent operator procedure for implicit elastoplastic BEM analysis", *Comput. Model. Eng. Sci.*, **6**(5), 431-439.
Olesen, J.F., Ostergaard, L. and Stang, H. (2005), "Nonlinear fracture mechanics and plasticity of the split cyliner test", *Mater. Struct.*, **39**(4), 421-432.
Peng, Q. and Chen, M.X. (2012), "An efficient return mapping algorithm for general isotropic elastoplasticity in principal space", *Comput. Struct.*, **92-93**, 173-184.
Pramono, E. and Willam, K. (1989), "Fracture energy-based plasticity formulation of plain concrete", *J. Eng. Mech. - ASCE*, **115**(5), 183- 1204.
Ribeiro, F. and Ferreira, I. (2007), "Parallel implementation of the finite element method using compressed data structures", *Comput. Mech.*, **41**(1), 31-48.
Rocco, C., Guinea, G.V., Palnas, J. and Elices, M. (1999), "Size effect and boundary conditions in the brazilian test: theoretical analysis", *Mater. Struct.*, **32**(6), 437-444.
Simo, J.C. and Taylor, R.L. (1985), "Consistent tangent operators for rate-independent elastoplasticity", *Comput. Method. Appl. M.*, **48**(1), 101-118.
Wilkins, M.L. (1963), *Calculation of Elastic–Plastic Flow*, University of California, Livermore, CA, USA.